Granular Tau Oligomers as Intermediates of Tau Filaments†

Sumihiro Maeda,‡ Naruhiko Sahara,‡ Yuko Saito,§ Miyuki Murayama,‡ Yuji Yoshiike,‡ Hyonchol Kim,||,⊥ Tomohiro Miyasaka,‡ Shigeo Murayama,§ Atsushi Ikai,|| and Akihiko Takashima*,‡

Lab for Alzheimer's Disease, RIKEN Brain Science Institute, 2-1 Hirosawa, Wako, Saitama 351-0198, Japan, Department of Neuropathology and Department of Pathology, Tokyo Metropolitan Institute of Gerontology, Tokyo Metropolitan Geriatric Hospital, 35-2 Sakaecho, Itabashi-ku, Tokyo 173-0015, Japan, and Department of Life Science, Graduate School of Bioscience and Biotechnology, Tokyo Institute of Technology, 4259 Nagatsuda, Midori-ku, Yokohama, Kanagawa 226-8501, Japan

Received July 6, 2006; Revised Manuscript Received December 15, 2006

ABSTRACT: Neurofibrillary tangles (NFTs) are pathological hallmarks of several neurodegenerative disorders, including Alzheimer's disease (AD). NFTs are composed of microtubule-binding protein tau, which assembles to form paired helical filaments (PHFs) and straight filaments. Here we show by atomic force microscopy that AD brain tissue and in vitro tau form granular and fibrillar tau aggregates. CD spectral analysis and immunostaining with conformation-dependent antibodies indicated that tau may undergo conformational changes during fibril formation. Enriched granules generated filaments, suggesting that granular tau aggregates may be an intermediate form of tau fibrils. The amount of granular tau aggregates was elevated in prefrontal cortex of Braak stage I cases compared to that of Braak stage 0 cases, suggesting that granular tau aggregation precedes PHF formation. Thus, granular tau aggregates may be a relevant marker for the early diagnosis of tauopathy. Reducing the level of these aggregates may be a promising therapy for tauopathies and for promoting healthy brain aging.

Neurofibrillary tangles (NFTs)[1] are common in many neurodegenerative diseases and to some degree in normal aging (*1*, *2*). NFTs are intracellular neuronal clusters of fibrils that consist of paired helical filaments (PHFs) and straight filaments (SFs). These filaments are composed of hyperphosphorylated tau, a type of microtubule-binding protein. Some have proposed a connection between NFT formation and neuronal loss, because NFTs are observed in brain regions that also exhibit neuronal loss (*3*). Recent genetic studies of frontotemporal dementia with parkinsonism linked to chromosome 17 (FTDP-17) revealed that a mutation in the tau gene induces NFT formation and neuronal loss (*4*), suggesting that tau dysfunction itself could lead to NFT formation and neuronal loss.

It is unclear, however, how tau forms fibrils and how tau contributes to neurodegeneration. A recent report showed that inhibiting tau expression in tau transgenic mice protected against neuronal death, even though NFTs were still produced (*5*). These results suggest that the degenerating pathway, triggered by tau overexpression, may branch from a tau filament formation pathway. Tau may produce toxic aggregates before forming tau fibrils.

Tau fibril formation has been studied extensively in vitro. Anionic surfactants accelerate fibril formation of tau protein in vitro (*6*). Fibril formation can be monitored by thioflavin fluorescence, which recognizes aggregations having a β-sheet conformation. In this study, together with the thioflavin assay, we applied atomic force microscopy (AFM) to tau in solution to track structural changes in tau and to identify intermediates of tau filaments.

MATERIALS AND METHODS

Expression and Purification of Recombinant Tau Protein. Recombinant human tau (2N4R) in the pRK172 vector was purified using methods described previously (*7*) with some modifications. Details of these methods are described in the Supporting Information. After being freeze-dried, tau was dissolved in water and stored as a stock solution at −30 °C.

Incubation of Tau and Fluorescence Spectroscopy (ThT assay). The degree of tau aggregation was determined using thioflavin T (ThT) (*8*). Tau or BSA (control protein) stock solutions were diluted to 10 μM with 10 mM HEPES (pH 7.4), 100 mM NaCl, 10 μM heparin, and 10 μM ThT (final volume of 50 μL per well) and incubated in a damp box at 37 °C. At indicated time points (see Figure 2), we measured ThT fluorescence levels as previously described (*9*).

Atomic Force Microscopy (AFM). A multimode Nanoscope IIIa (Digital Instruments, Santa Barbara, CA) equipped

† This work is partly supported by a Grant-in-Aid for Scientific Research (11680746, from the Japanese Ministry of Education, Science, and Culture) and Promotion of Novel Interdisciplinary Fields Based on Nanotechnology and Materials.

* To whom correspondence should be addressed. E-mail: kenneth@brain.riken.jp. Telephone: +81-(0)48-467-9627. Fax: +81-(0)48-467-5916.

‡ RIKEN Brain Science Institute.

§ Tokyo Metropolitan Geriatric Hospital.

|| Tokyo Institute of Technology.

⊥ Present address: Department of Biomedical Information, Division of Biosystems, Institute of Biomaterials and Bioengineering, Tokyo Medical and Dental University, 2-3-10 Surugadai, Chiyoda-ku, Tokyo 101-0062, Japan.

[1] Abbreviations: NFT, neurofibrillary tangle; PHF, paired helical filament; SF, straight filament; FTDP-17, frontotemporal dementia with parkinsonism linked to chromosome 17; AFM, atomic force microscopy; dLLS, dynamic laser light scattering; sLLS, static laser light scattering; CD, circular dichroism; ThT, thioflavin T; BSA, bovine serum albumin.

10.1021/bi061359o CCC: $37.00
Published on Web 03/06/2007

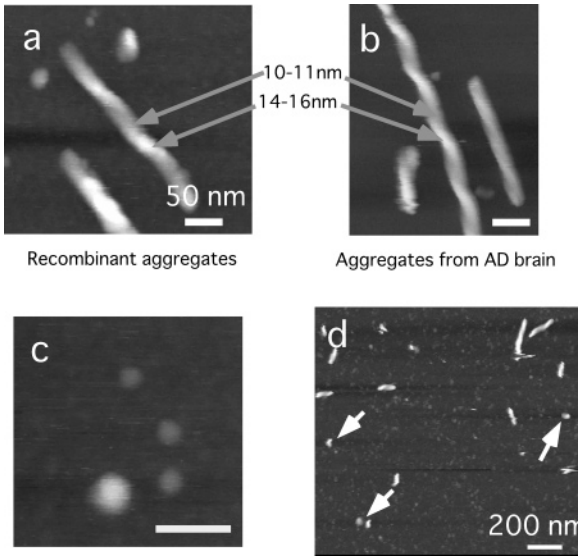

FIGURE 1: AFM images of recombinant tau aggregates in solution, fibrils (a) and granules (c). AFM images of PHFs and straight filaments purified from an AD brain (b). The heights of "mountains and valleys" of the twisted filaments are indicated. Tau-enriched fractions from the AD brain contain tau fibrils and granules (arrow) (d). Scale bars are 50 (a−c) and 200 nm (d).

with tapping mode was used for AFM observations in solution. An OMCL-TR400PSA device (Olympus) was used as a microcantilever. Incubated tau solutions from three different Black Cliniplate wells were combined, dropped onto freshly cleaved mica, allowed to set for 10 min, and then examined via AFM. For human tau, samples were left on the mica surface for 30 min and washed once with buffer prior to AFM assessment. We processed the height images of structures using NIH-image 1.62 and calculated the major (length) and minor (diameter) axes for each particle. Data from four different regions (4 μm^2) of each structure were plotted.

Sucrose Step Gradients and Preparation of Concentrated Tau. An incubated or immunoaffinity-purified tau solution (1 mL) was fractionated using discontinuous sucrose gradients using a TLA 55 rotor (Beckman) on a 5 mL scale as described previously (*10*). To concentrate the fractions and for buffer exchanges with 10 mM HEPES and 100 mM NaCl, we filtered the fractions using Centricut mini filters (10 kDa cutoff; KURABOU) at room temperature for 1 or 2 days. Although granular tau oligomers are insoluble in sarcosyl (Figure 1 of the Supporting Information), most remained in the supernatant fraction after ultracentrifugation (100K*g* for 30 min) because of their small sedimentation coefficient. Centrifuging the supernatant fraction at 200K*g* for 2 h, however, successfully separated the oligomers from soluble and flexible tau species.

Dot Blot Analysis. The tau protein concentration in each fraction was determined using amino acid hydrolysis, and the same amount of tau was dotted onto nitrocellulose membranes. We used the following primary antibodies: E1 (recognizes total tau), MC1 (recognizes PHF tau conformational change; generous gift from P. Davies, Albert Einstein College of Medicine, Bronx, NY), and A11 (recognizes the conformation of toxic Aβ; Biosource) (*11*). The membranes were incubated with peroxidase-labeled secondary antibody and visualized using ECL.

Laser Light Scattering and Circular Dichroism Spectroscopy. The buffers from fractions 1 and 3 were exchanged with high-salt buffer [10 mM Tris (pH 7.4) and 800 mM NaCl] to minimize further aggregation. To ensure the elimination of filaments formed in the filtering step, the sample was centrifuged at 100K*g* for 30 min at 4 °C. After we had confirmed that the granular aggregates were not filamentous using AFM, the tau oligomeric fraction was subjected to static and dynamic laser light scattering using a Zetasizer (Sysmex) at 23 °C. The molecular mass of granular tau oligomer was calculated as the average of triplicate experiments.

We measured the circular dichroism (CD) spectra of each fraction with a J-720 spectropolarimeter (Jasco). Samples placed in a cuvette with a path length of 1 mm were measured from 200 to 260 nm at 23 °C. Spectra obtained from an average of 20 scans were converted to mean residue ellipticity.

Human Brain Sample Preparation. Granular tau oligomer fractions from human brains were purified according to procedures described previously (*10*). Significant differences between each Braak stage were tested with the Kruskal Wallis test. Data were analyzed with InStat 3 for Macintosh (Graphpad, San Diego, CA).

RESULTS

Assessing the Formation of Filaments and Granules by AFM. AFM examination of a tau solution incubated for 72 h revealed the presence of twisted filaments (Figure 1a) resembling PHFs (Figure 1b). This experimental system allowed us to observe both filament and granule formation (Figure 1a,c). AFM examination of immunoaffinity-purified tau from AD brains revealed granules that are the same size as those observed in the in vitro tau aggregation system (Figure 1d). Granules and tau filaments were insoluble in *N*-lauroylsarcosine (sarcosyl) detergent (Figure 1 of the Supporting Information). These observations suggest that tau aggregates may form two different structures, granules and fibrils, both in vitro and in vivo.

Granule Formation Precedes Filament Formation. To understand the relationship between these different tau aggregates, we investigated how tau assembly in vitro changes over time by measuring ThT fluorescence and by using AFM. During the first incubation period of 4 h, ThT fluorescence levels remained constant and no aggregates were observed via AFM (Figure 2a of the Supporting Information). After incubation for 4 h, however, ThT fluorescence levels increased and spherically or elliptically shaped granules and fibrils formed (Figure 2a,b of the Supporting Information). We used the major-to-minor axis ratio to define granules ($1 \leq$ major-to-minor axis ratio < 2) and fibrils ($2 \leq$ major-to-minor axis ratio) and then determined temporal changes in ThT fluorescence (Figure 2). At incubation for 6 h, granule levels increased rapidly, reaching a plateau at 21 h. After incubation for 21 h, even though the levels of granular tau oligomers had plateaued, tau fibrils continued to grow. The number and length of fibrils continued to increase with incubation times of up to 328 h, reaching lengths of up to 950 nm and diameters of 15−25 nm (Figure 2c of the Supporting Information).

ThT fluorescence intensity seemed to correspond to both granular and fibrillar tau levels, suggesting that both granules

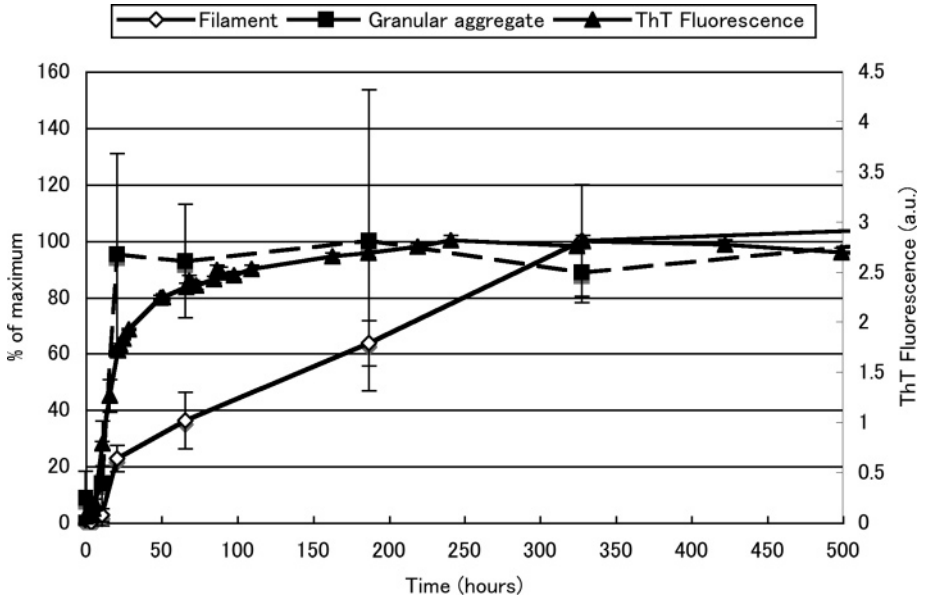

FIGURE 2: Temporal changes in ThT fluorescence and in granular tau oligomer and tau fibril levels. The ThT fluorescence of tau aggregation was measured at the indicated time points (mean ± standard deviation; $n = 3$). Tau granule and fibril levels were determined by calculating the area occupied from AFM images of tau samples taken at each time point (Figure 2b,c of the Supporting Information). Data are represented as percentages of the maximum oligomer and fibril levels (mean ± standard deviation).

and fibrils may possess a β-sheet conformation. These results led us to conclude that the granular tau oligomer might represent an intermediate form of tau fibril.

Characterization of Granular Tau Aggregates. We characterized granular tau aggregates by separating granular tau oligomers from the tau aggregate mixture. We then fractionated the incubated sample using sucrose gradient ultracentrifugation (Figure 3a). While fraction 1 contained no apparent aggregate, fraction 3 contained the largest amounts of granular tau oligomers. The size of granules in fraction 3 was normally distributed, with the largest sizes reaching 15−25 nm, as determined by AFM. Fractions 4−6 contained filaments. Since we could not assess by AFM the contamination of fraction 3 with soluble tau, we employed dynamic laser light scattering (dLLS) to assess soluble tau. dLLS analysis of fraction 3 revealed a single-peak distribution distinct from that of soluble tau (Figure 3b). Therefore, we concluded that fraction 3 does not contain fibrils or soluble tau but instead contains granular tau aggregates.

The temporal change of tau levels in each fraction was investigated using CBB staining after electrophoresis. In fraction 1 (soluble tau fraction), the amount of tau was reduced, corresponding to an increasing level of granular tau oligomer and fibril formation; tau levels in fraction 3 (granular tau oligomer fraction) decreased at later stages of the incubation, while the tau level in fraction 6 (filament fraction) continuously increased (Figure 3 of the Supporting Information). This result supports the observation under AFM that granular tau oligomer may be an intermediate form for tau filament.

We used fraction 3 to determine an approximate molecular mass of the granular tau oligomer. Figure 3c shows a Debye plot obtained from static laser light scattering (sLLS) analysis of granular oligomeric tau. The KC/RoP value at the *y*-intercept (sample concentration of zero) equals the reciprocal of the approximate molecular mass of the granular tau oligomer (Figure 3c). The approximate molecular mass of the granular tau oligomer averaged 1843.3 ± 112.4 kDa (average ± standard deviation; $n = 3$ replications), corresponding to 40 ± 3 tau molecules. KC/RoP values decreased as the sample concentration increased; that is, the granular tau oligomer has a negative second virial coefficient indicative of adhesive properties (*12*).

Conformational Differences between Granular and Fibrillar Tau. We used circular dichroism (CD) spectral analysis to analyze structural differences between soluble (fraction 1), granular oligomeric (fraction 3), and fibrillar forms (pellet, fraction 6) of tau. The spectral curve of fraction 1 had a minimum ellipticity of approximately 200 nm, indicating a random coil structure (*13*). Fibrillar tau (fraction 6) had fewer random coil structures and a growing "shoulder" in the curve at ~220 nm, indicating β-sheet structure. The CD spectrum of the granular tau oligomer (fraction 3) also revealed a shoulder smaller than that of fibrillar tau at ~220 nm (Figure 3d). The CD spectrum of granular tau oligomers was distinct but intermediate in form compared to those of soluble and fibrillar tau, suggesting that the granular tau oligomer may represent an intermediate structure. This observation was confirmed by probing samples of each tau fraction with conformation-dependent antibodies (Figure 3e). E1 antibody, which recognizes the N-terminus of tau, immunostained all fractions to the same extent. MC1, which recognizes a conformational change in PHF, did not immunostain the soluble tau fraction (fraction 1) but did immunostain granular and fibrillar tau fractions (fractions 2−6). A11 antibody, which recognizes toxic oligomers of β-amyloid, immunostained only fibrillar fractions (fractions 4−6). Taken together, these results indicate that tau fibrils might have another conformational form having an additional structure distinct from that of granular tau oligomer.

Conversion of Granular Aggregates into Filaments. To examine whether granular tau aggregates could form filaments, we enriched the concentration of tau by filtering fractions 1 and 3. Samples containing enriched granular tau oligomer formed filaments (Figure 4c,d), while samples containing enriched soluble tau failed to form aggregates

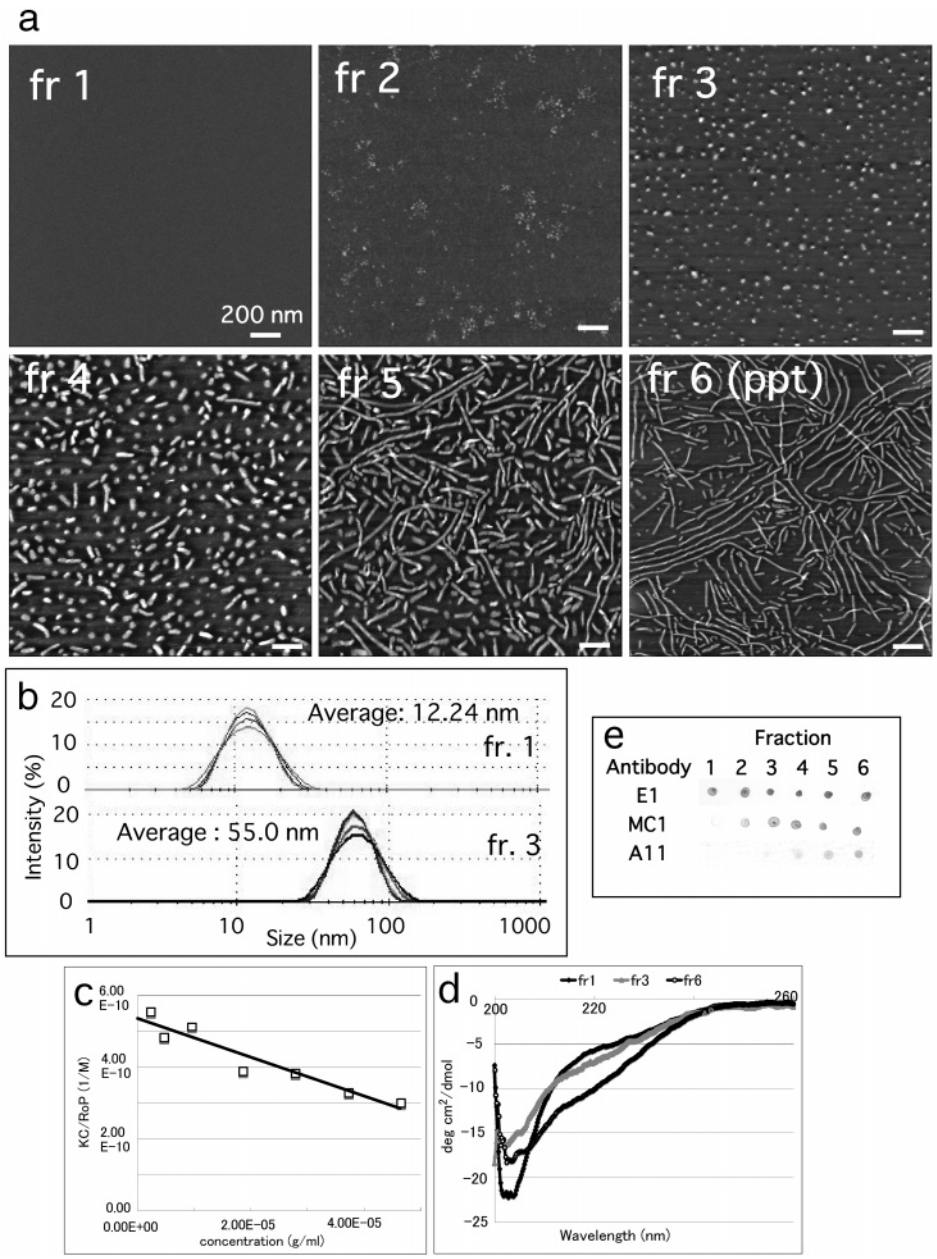

FIGURE 3: Purification and characterization of granular tau oligomers. (a) AFM images of fractions after sucrose gradient centrifugation. The scale bar is 200 nm. (b) Size distribution of soluble tau (fraction 1) and granular tau (fraction 3) as determined by dynamic laser light scattering. Fraction 1 displayed a distribution similar to that of monomeric tau species. Fraction 3, however, displayed a distribution of structures distinct from that of fraction 1, indicating that nonaggregated tau species do not contaminate fraction 3. (c) Analysis of the granular tau oligomer fraction using static laser light scattering. Debye plot of KC/RoP for different tau concentrations (□). The *y*-intercept value of the best linear fit indicates the approximate reciprocal of the molecular mass of granular oligomeric tau. (d) CD spectrum of fractions 1 (soluble tau oligomer), 3 (granular tau oligomer), and 6 (tau fibril). (e) The same amount of tau in each fraction was dotted onto nitrocellulose membranes and probed with the indicated antibodies.

(Figure 4a,b). These results strongly suggest that tau fibrils stem from granular tau oligomers or, in other words, that the granular tau oligomer is an intermediate form of tau fibril.

To confirm that granular tau aggregates form before the formation of tau fibrils in vivo, we purified, by immunoaffinity purification and sucrose gradient centrifugation, granular tau aggregates from human frontal cortex of cases evaluated to be at different Braak stages. As with the recombinant tau aggregation experiment, we detected granular tau oligomers in fraction 3 (Figure 4 of the Supporting Information) derived from Braak stage V samples (which have NFTs) (Figure 4e). Then, we could also detect them in fraction 3 derived from Braak stage 0 samples (which have no NFTs) (Figure 4e). The amount of granules in the Braak stage 0 samples, however, was significantly low. We also examined PHF-tau in Braak stage 0, I, III, and V samples by using a precipitation method (*14*) and found high levels of PHF-tau in Braak stage V brains but no detectable levels of PHF-tau in Braak stage 0, I, and III brains (*10*). These observations are consistent with the pathological evaluations of these brains.

Quantitative analysis showed increased levels of granular tau even in samples at Braak stage I, a stage characterized by the lack of NFTs in the frontal cortex. This finding suggests that tau granules accumulate far before tau fibrils form. Similar to what we found in our in vitro tau aggregation

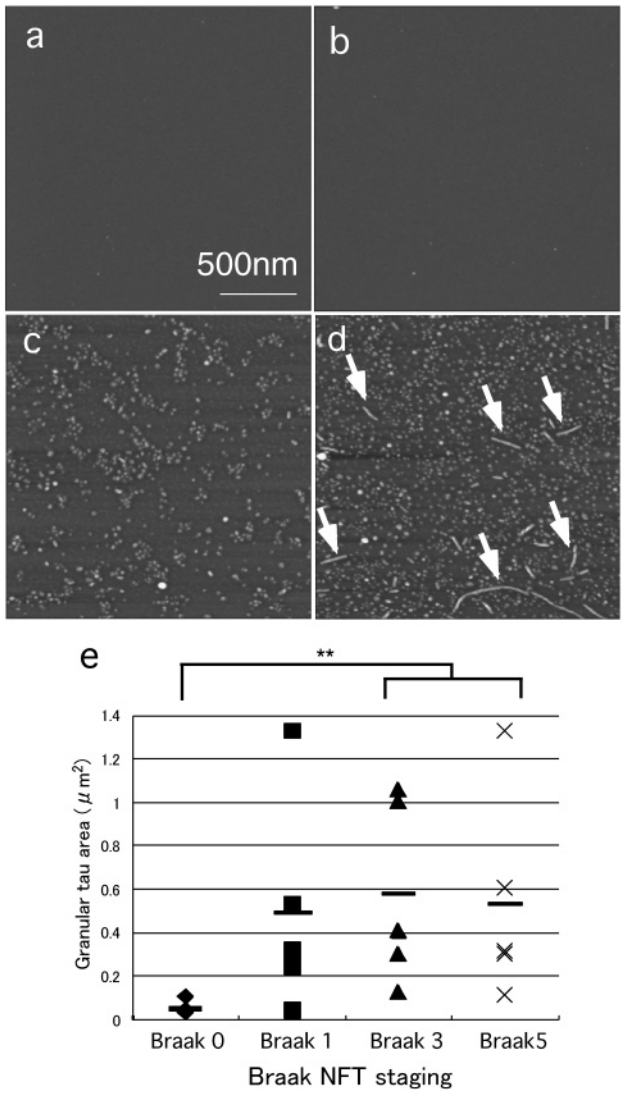

FIGURE 4: Tau filaments generated from granular tau oligomers. (a−d) AFM images of fractions 1 (a and b) and 3 (c and d), before (a and c) and after (b and d) the samples had been concentrated in the absence of heparin. Although concentrated fraction 1 had no structures, concentrated fraction 3 generated filaments (arrows). (e) The granular tau oligomer was purified as described in Materials and Methods from pathologically staged frontal cortex samples. Quantitative measurements of tau present in fraction 3 were derived from NIH-image 1.62 and are represented as the area (square micrometers) occupied by tau granules Two asterisks denote $p = 0.0155$ (Kruskal Wallis test).

experiments, high concentrations of granular tau oligomers in vivo may also lead to tau fibril formation in the brains of individuals with AD. Thus, granular tau oligomers may also represent an intermediate structure of tau during tau fibril formation in the human brain.

DISCUSSION

Tau Filaments Develop from Granular Tau Oligomers. Here we report that 40mer tau oligomers form granular structures having an MC1 epitope, indicating that this granular tau oligomer consists of conformationally changed tau. Partially folded tau monomers that are distinct from native tau monomers and that display a reduced level of random coiling but an increased level of β-sheet conformation have been reported previously (*15*). This type of conformation is similar to that displayed by granular tau oligomers; therefore, granular oligomers may be composed of these monomers.

Fibrils have a tendency to take on β-sheet conformations and also stain positively for anti-oligomer A11 antibody (*11*), which is consistent with our finding that A11 specifically recognizes proteins having either β-barrel or β-sandwich structures (Y. Yoshiike and A. Takashima, unpublished data). Therefore, tau fibrils may be composed of an assembly of granular tau aggregates having a β-sheet structure. Smaller granules of tau oligomers may grow by binding with soluble tau. Once the oligomer reaches a size of 20 nm, binding of granular tau oligomers enables tau fibrils to develop. This premise is consistent with our observation that only granular tau oligomers were detectable in the early stages of incubation, and the fact that fibrils appeared after longer incubations and CBB staining after electrophoresis in each fraction also support this idea (Figure 3 of the Supporting Information). After incubation for 7 months (5500 h), all tau monomers and granular tau oligomers had converted into filaments (data not shown). These observations are consistent with our hypothesis that the granular tau oligomer represents an intermediate form of tau filament.

In prions, complex pathways determine whether monomers derived from dissociated oligomers convert into filaments (*16*). Using our recombinant tau aggregation system, we examined fraction 3 to determine whether tau oligomers dissociate to form monomers, but we found no monomer contamination in fraction 3 (Figure 3b). After concentrating soluble tau and granular tau fractions (fractions 1 and 3, respectively), we found that granular tau, not soluble tau, is capable of forming filaments without additional heparin. This indicated that granular tau represents an intermediate form but that soluble tau does not. The mechanism underlying filament elongation by binding of granular tau oligomer needs further clarification.

Granular Tau Oligomers in Human Brain. Granular tau oligomers have been found in human brains. These oligomers consist of highly phosphorylated tau and are similar in size to granular tau oligomers derived from recombinant tau (*10*). PHFs could also be broken down into granular tau oligomers as well as filaments derived from recombinant protein (Figure 5a,b of the Supporting Information), further confirming the intermediary role of the granular tau oligomer during PHF formation in the human brain.

In the aged brain, PHF formation may occur when the level of granular tau oligomers increases. Although we found that non-AD brains contained no histologically verified NFTs, these brains did contain granular tau oligomers, albeit fewer than did AD brains. Interestingly, we also detected increased granular tau oligomer levels in brains showing early stage tau pathology. This was consistent with our immunochemical findings showing that granular tau oligomers are immunoreactive for MC1, which was recently reported to be a good indicator of early stage tau pathology in the frontal gyrus, even in the absence of NFTs (*17*). These biochemical data suggested that the formation of a granular tau oligomer precedes NFT formation. Moreover, we found significant differences in the number of granular tau oligomers in Braak stage 0 and I brains (*10*) but not in an oligomer-occupied area per field. We did find, however, significant differences

in oligomer areas in Braak stage 0, III, and V brains, indicating that the oligomers in Braak stage I brains are smaller than those in Braak stage III or V brains. Indeed, in one Braak stage I case that contained a large number of granular tau oligomers, we found smaller-sized granules (data not shown).

Recent results have shown that inhibiting tau expression halfway during the neurodegeneration process in tau transgenic mice induces NFT formation without producing neuronal death (*5*). The findings presented here are not sufficient to resolve this issue. We do know, however, that tau overexpression in tau transgenic mice and in AD brains increases granular tau levels, ultimately leading to NFT formation and neuronal death (*18*−*21*). If the threshold concentration of granular tau that leads to neuronal death is higher than concentrations that lead to NFT formation, inhibiting tau expression could prevent neuronal death, even though NFTs are still generated. If this assumption is true, reducing oligomeric tau might be a promising therapy for various tauopathies, including those associated with aging. Nevertheless, the toxic nature of granular oligomeric tau aggregates needs to be further assessed.

ACKNOWLEDGMENT

We thank Dr. Hara for permitting us to use the NanoscopeIIIa, Drs. Kobayashi and Hayakawa for permitting us to use the Zetasizer, Mr. Usui and Miss Ohtsuki for MS spectroscopy, and Mr. Morishita for amino acid hydrolysis.

SUPPORTING INFORMATION AVAILABLE

Sarcosyl insoluble tau aggregates (Figure 1), temporal changes in in vitro tau aggregation (Figures 2 and 3), details of granular tau oligomer purification from human brain (Figure 4), and tau filament breakdown by continuous AFM imaging (Figure 5). This material is available free of charge via the Internet at http://pubs.acs.org.

REFERENCES

1. Braak, H., and Braak, E. (1997) Frequency of stages of Alzheimer-related lesions in different age categories, *Neurobiol. Aging 18*, 351−357.
2. Lee, V. M., Goedert, M., and Trojanowski, J. Q. (2001) Neurodegenerative tauopathies, *Annu. Rev. Neurosci. 24*, 1121−1159.
3. Ihara, Y. (2001) PHF and PHF-like fibrils: Cause or consequence? *Neurobiol. Aging 22*, 123−126.
4. Reed, L. A., Wszolek, Z. K., and Hutton, M. (2001) Phenotypic correlations in FTDP-17, *Neurobiol. Aging 22*, 89−107.
5. Santacruz, K., Lewis, J., Spires, T., Paulson, J., Kotilinek, L., Ingelsson, M., Guimaraes, A., DeTure, M., Ramsden, M., McGowan, E., Forster, C., Yue, M., Orne, J., Janus, C., Mariash, A., Kuskowski, M., Hyman, B., Hutton, M., and Ashe, K. H. (2005) Tau suppression in a neurodegenerative mouse model improves memory function, *Science 309*, 476−481.
6. Barghorn, S., and Mandelkow, E. (2002) Toward a unified scheme for the aggregation of tau into Alzheimer paired helical filaments, *Biochemistry 41*, 14885−14896.
7. Hasegawa, M., Smith, M. J., and Goedert, M. (1998) Tau proteins with FTDP-17 mutations have a reduced ability to promote microtubule assembly, *FEBS Lett. 437*, 207−210.
8. Friedhoff, P., Schneider, A., Mandelkow, E. M., and Mandelkow, E. (1998) Rapid assembly of Alzheimer-like paired helical filaments from microtubule-associated protein tau monitored by fluorescence in solution, *Biochemistry 37*, 10223−10230.
9. Yoshiike, Y., Tanemura, K., Murayama, O., Akagi, T., Murayama, M., Sato, S., Sun, X., Tanaka, N., and Takashima, A. (2001) New insights on how metals disrupt amyloid β-aggregation and their effects on amyloid-β cytotoxicity, *J. Biol. Chem. 276*, 32293−32299.
10. Maeda, S., Sahara, N., Saito, Y., Murayama, S., Ikai, A., and Takashima, A. (2006) Increased levels of granular tau oligomers: An early sign of brain aging and Alzheimer's disease, *Neurosci. Res. 54*, 197−201.
11. Kayed, R., Head, E., Thompson, J. L., McIntire, T. M., Milton, S. C., Cotman, C. W., and Glabe, C. G. (2003) Common structure of soluble amyloid oligomers implies common mechanism of pathogenesis, *Science 300*, 486−489.
12. George, A., and Wilson, W. W. (1994) Predicting protein crystallization from a dilute solution property, *Acta Crystallogr. D50*, 361−365.
13. Schweers, O., Schonbrunn-Hanebeck, E., Marx, A., and Mandelkow, E. (1994) Structural studies of tau protein and Alzheimer paired helical filaments show no evidence for β-structure, *J. Biol. Chem. 269*, 24290−24297.
14. Greenberg, S. G., and Davies, P. (1990) A preparation of Alzheimer paired helical filaments that displays distinct tau proteins by polyacrylamide gel electrophoresis, *Proc. Natl. Acad. Sci. U.S.A. 87*, 5827−5831.
15. Chirita, C. N., Congdon, E. E., Yin, H., and Kuret, J. (2005) Triggers of full-length tau aggregation: A role for partially folded intermediates, *Biochemistry 44*, 5862−5872.
16. Baskakov, I. V., Legname, G., Baldwin, M. A., Prusiner, S. B., and Cohen, F. E. (2002) Pathway complexity of prion protein assembly into amyloid, *J. Biol. Chem. 277*, 21140−21148.
17. Haroutunian, V., Davies, P., Vianna, C., Buxbaum, J. D., and Purohit, D. P. (2005) Tau protein abnormalities associated with the progression of alzheimer disease type dementia, *Neurobiol. Aging* (in press).
18. Tatebayashi, Y., Miyasaka, T., Chui, D. H., Akagi, T., Mishima, K., Iwasaki, K., Fujiwara, M., Tanemura, K., Murayama, M., Ishiguro, K., Planel, E., Sato, S., Hashikawa, T., and Takashima, A. (2002) Tau filament formation and associative memory deficit in aged mice expressing mutant (R406W) human tau, *Proc. Natl. Acad. Sci. U.S.A. 99*, 13896−13901.
19. Tanemura, K., Akagi, T., Murayama, M., Kikuchi, N., Murayama, O., Hashikawa, T., Yoshiike, Y., Park, J. M., Matsuda, K., Nakao, S., Sun, X., Sato, S., Yamaguchi, H., and Takashima, A. (2001) Formation of filamentous tau aggregations in transgenic mice expressing V337M human tau, *Neurobiol. Dis. 8*, 1036−1045.
20. Tanemura, K., Murayama, M., Akagi, T., Hashikawa, T., Tominaga, T., Ichikawa, M., Yamaguchi, H., and Takashima, A. (2002) Neurodegeneration with tau accumulation in a transgenic mouse expressing V337M human tau, *J. Neurosci. 22*, 133−141.
21. Brandt, R., Hundelt, M., and Shahani, N. (2005) Tau alteration and neuronal degeneration in tauopathies: Mechanisms and models, *Biochim. Biophys. Acta 1739*, 331−354.

BI061359O